Materials Research Letters

ISSN: (Print) (Online) Journal homepage: https://www.tandfonline.com/loi/tmrl20

Revealing the mechanical behavior of homogeneous dislocation cell units in high-entropy alloy

Liangxue Zhang, Qingsong Pan & Lei Lu

To cite this article: Liangxue Zhang, Qingsong Pan & Lei Lu (2023) Revealing the mechanical behavior of homogeneous dislocation cell units in high-entropy alloy, Materials Research Letters, 11:11, 907-914, DOI: 10.1080/21663831.2023.2256359

To link to this article: https://doi.org/10.1080/21663831.2023.2256359

MATER. RES. LETT.
2023, VOL. 11, NO. 11, 907–914
https://doi.org/10.1080/21663831.2023.2256359

MATERIALS RESEARCH LETTERS
Taylor & Francis
Taylor & Francis Group

ORIGINAL REPORTS

Revealing the mechanical behavior of homogeneous dislocation cell units in high-entropy alloy

Liangxue Zhang[a,b]*, Qingsong Pan[a]* and Lei Lu[a]

[a]Shenyang National Laboratory for Materials Science, Institute of Metal Research, Chinese Academy of Sciences, Shenyang, People's Republic of China; [b]School of Materials Science and Engineering, University of Science and Technology of China, Shenyang, People's Republic of China

ABSTRACT

Gradient dislocation cell structured $Al_{0.1}CoCrFeNi$ high-entropy alloys exhibited exceptional strength and uniform ductility. HEA containing homogeneous dislocation cells, with the average size varying from 0.29 to 0.43 μm was observed to still exhibit a superior combination of high strength and good uniform elongation, distinct from traditional strong ultrafine-grained structures with limited ductility. This is because the initial dislocation cells tend to be progressively patterned into dense dislocation walls upon straining, associated with the massive dislocation motion and accumulation. The gradient-induced additional strain hardening behavior was clarified by directly comparing the mechanical behavior of the homogeneous and gradient samples.

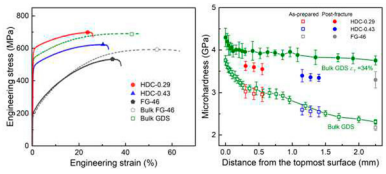

ARTICLE HISTORY
Received 5 July 2023

KEYWORDS
HEA; homogeneous dislocation cell; deformation behavior; strain hardening

IMPACT STATEMENT

Both high strength and good ductility can be simultaneously achieved in homogeneous ultrafine-sized dislocation cell, distinct from traditional strong, yet less ductile ultrafine-grained structures.

1. Introduction

Significantly improving the strength of metallic materials has been a central issue in materials science over the past century, but is also critical to the development of high-performance structural components that improve service safety and energy efficiency in the face of the current energy crisis and global warming challenges [1]. Since line defects, i.e. full dislocations, act as the basic plastic strain carriers, conventional strengthening methodologies usually strongly resist the motion and transmission of full dislocations by generating various defects [1–4].

One well-known strategy is structural modification, involving the incorporation of a high density of high-angle grain boundaries (GBs) with misorientation angles larger than 15° into the crystalline lattice, commonly referred to as the nanograined or ultrafine-grained (UFG) structure [5]. Indeed, the resultant metals and alloys with homogeneous ultrafine and nanosized grains possess very high strength, but inevitably become brittle and show limited tensile ductility (a few percent) prior to catastrophic failure, even in the case of metals that are ductile in their coarse-grained (CG) forms, such as copper and aluminum [6–8]. The tensile brittleness in nanostructured metals mainly arises from the absence of work-hardening of nanosized grains, as the conventional process of dislocation slip and storage is substantially suppressed within the extremely tiny grains without slip transmission across high-angle GBs [6–8].

In the past decade, significant advances have been made in engineering materials with architectural heterostructures, particularly gradient nanostructures containing spatially graded structural components with

CONTACT Lei Lu llu@imr.ac.cn Shenyang National Laboratory for Materials Science, Institute of Metal Research, Chinese Academy of Sciences, Shenyang 110016, People's Republic of China

*These authors contributed equally.

highly variable length scales, most of which exhibit unprecedented mechanical properties, such as improved strength-ductility combinations and extraordinary strain hardening [9–17]. The gradient nanograined (GNG) Cu, having the grain size spatially graded distributed from nanoscale in the surface to micrometer in substrate, was found to show a twice yield stress while maintaining a comparable tensile ductility, relative to the CG substrate ($\sim$31%). Similar results were also identified in other GNG metals and alloys, such as Ni, 316 steels, etc. [9,12,13]. The work hardening and tensile plasticity of global GNG samples are mainly determined by their CG substrate, owing to the fact that the free-stranding GNG surface foils have a high strength, yet very limited uniform elongation (commonly $<2\%$), analogous to conventional nanograined metals [6,9,13]. A unique deformation mechanism with mechanical-driven high-energy grain boundary migration process with grain growth or shear band in top surface GNG layer was proposed, which is an evidently softening process, thereby deteriorating the further property enhancements of GNG metals [9,13].

Recently, a sample-level gradient ultrafine-scaled low-angle dislocation-cell structure (GDS) was controllably introduced in 304 stainless steel [18] and high entropy alloy (HEA) by using a cyclic-torsion treatment (CT) without any surface tooling [19,20]. In particular, the initial grain size and morphology from the surface to the core are almost unchanged, fundamentally distinct from the GNG structure after surface mechanical treatments [9,13]. Specifically, GDS HEA displays a 3 times yield strength meanwhile maintaining steady work-hardening and a comparable tensile ductility after CT processing. Such an exceptional strength and ductility synergy is rarely achieved in homogeneous or heterogeneous structures and most existing GNG metals and alloys [9,19,21–24]. Massive stacking-faults are progressively activated to dominate the plastic deformation and also gradually cause a refinement of dislocation cells, thereby contributing to such a superior mechanical performance of GDS HEA [19,20]. Nevertheless, fundamental understanding of tensile behavior of gradient cell structured metallic materials is still in its infancy. For instance, whether the elementary structural unit of gradient dislocation structure, i.e. homogeneous dislocation cell pattern, tends to be either ductile or brittle is still an open question.

Recently, additively manufactured metals (such as stainless steel), usually composed of hierarchically heterogeneous microstructures, including massive solidification-induced dislocation cell pattern, low-angle grain boundaries and chemical heterogeneity, exhibit a combination of high yield strength and considerable tensile ductility simultaneously [25–27]. These cellular structures formed during the solidification, characterized by their absence of local misorientation at the cell walls, are believed to deviate from the conventional dislocation patterning typically generated through plastic deformation [26]. Despite sharing similar morphology, these structures differ fundamentally. Interestingly, the exceptional mechanical capabilities observed in additively manufactured metals suggest that the inherent dislocation patterns within them lean towards inherent ductility.

In this study, we performed tensile tests of almost homogeneous dislocation cell (HDC) units with two different cell sizes of 0.29 and 0.43 μm, that are controllably peeled from different positions of GDS sample. These HDC components are discovered not only strong, but also ductile, with a good uniform elongation larger than 24%, fundamentally distinct from the less ductile feature of conventional homogeneous ultrafine-grained structures.

2. Materials and methods

$Al_{0.1}$CoCrFeNi HEA ingots with a composition of 2.44Al-24.39Co-24.39Cr-24.39Fe-24.39Ni (at%) were produced by vacuum-induction melting and then homogenized at 1200°C for 5 h. Subsequently, these ingots with a large sized grain of $\sim$560 μm were further deformed by three directionally forging and annealed at 980°C for 1.5 h to obtain the homogeneous fine-grained (FG) sample with a grain size of $\sim$46 μm.

The cylindrical HEA specimens with a large gauge diameter of 9 mm and a long gauge length of 24 mm were cyclically torsioned on Instron 8874 testing machine with a torsion angle amplitude of 20° and a total torsion number of 200 cycles at ambient temperature. Parallel to the rod axial direction, several HDC plate foils with a dimension of 4.5 mm × 2.4 mm × 0.45 mm were controllably peeled by using an electrical spark machine, at different depth ranges of 0.6–1.2 mm, 1.8–2.4 mm from top surface and at the core. Next, the corresponding dog-bone-shaped HDC and FG tensile specimens with a final gauge section of 5 mm × 1.8 mm and a thickness of $\sim$0.25 mm were cut from these foils by using Femtosecond laser, respectively, as schematically shown in Figure 1(a). Finally, those samples were mechanically polished and then followed by electro-polishing under a voltage of 15 V for $\sim$30 s at room temperature. Those small homogeneous dog-bone plate tensile specimens are used to explore the mechanical behavior of typical free-standing structural components in gradient cell structure.

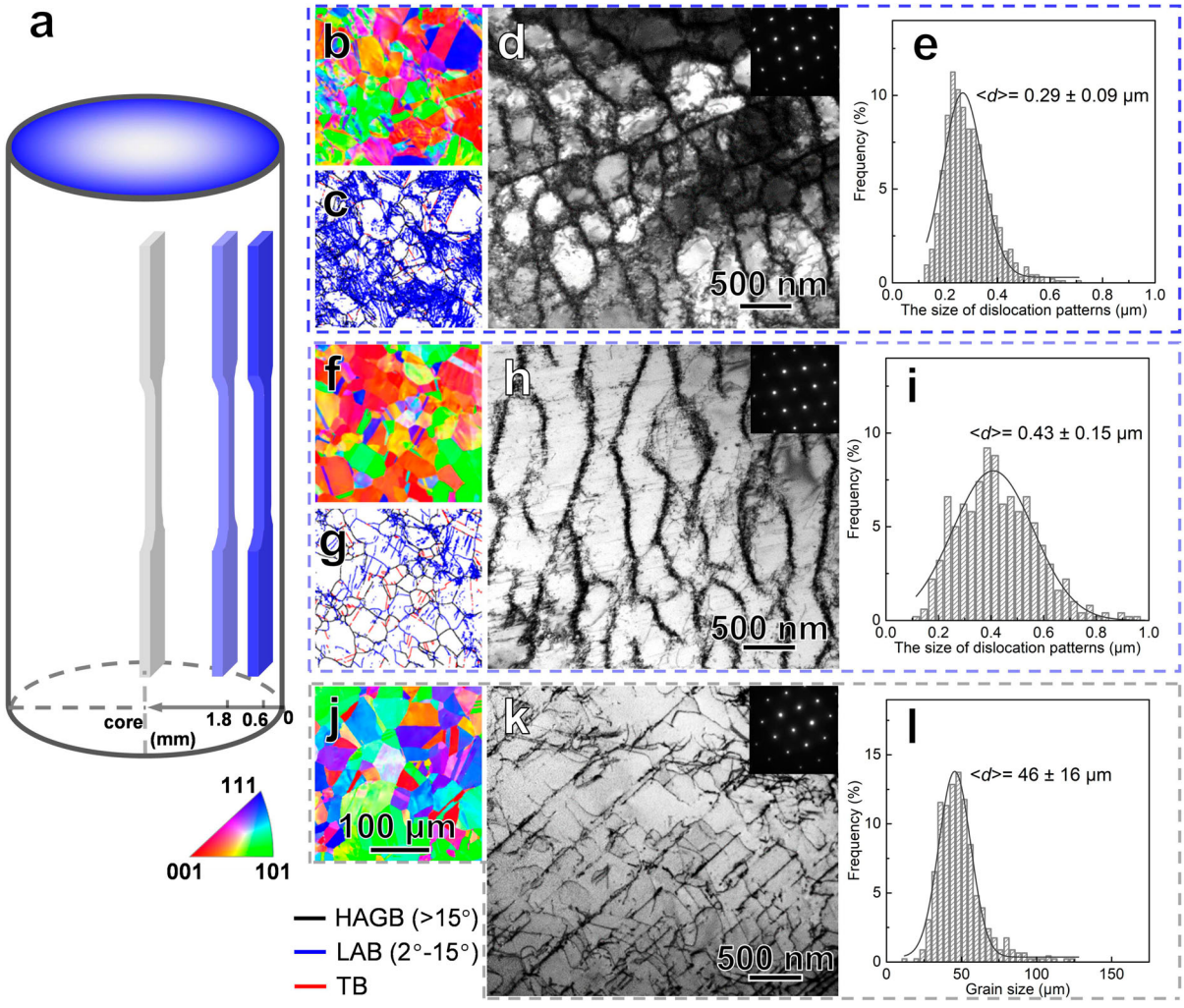

Figure 1. Preparation and microstructure of homogeneous dislocation cell (HDC) HEA samples. (a) Schematic showing plate dog-bone shaped HDC components cut from different depths of GDS sample prepared by CT treatment. The DS structure in surface is shown by blue and the core in gray. Cross-sectional EBSD images (b–c, f–g, j) showing the distribution of grain feature and three types of boundaries (HAGB, LAB, and TB) with different misorientation angles in HDC-0.29, HDC-0.43 and FG samples, respectively. Bright-field TEM images (d, h) and the corresponding statistic sizes (e, i), showing the typical dislocation pattern and size in both HDC-0.29, HDC-0.43 units. Bright-field TEM image (k) and the corresponding statistic size (i) showing the homogeneous FG with a relatively-low density of dislocations at the core.

Uniaxial tensile tests of HDC units were performed on Instron 68TM-5 microtester at room temperature at a strain rate of $5\times10^{-3}\,s^{-1}$. A contactless gauging system based on digital image correlation technique was used to monitor the tensile strain. At least three specimens were tested for repeatability.

The microstructure of HDC samples was characterized on scanning electron microscope (SEM) FEI Verios 460 using backscattering electron imaging mode, FEI Tecnai G2 F20 and FEI Titan Cubed Themis G2 60-300 transmission electron microscopes (TEM). The average structural size of HDC and FG units was obtained from more than 500 measurements. The electron backscatter diffraction analysis was performed on Zeiss Supra 55 SEM with a step size of 500 nm. Microhardness tests were conducted on Qness Q10A + microhardness tester with a load of 10 g and a holding time of 10 s; at least 10 measurements were averaged to obtain the values, while the error bar is the mean +/− standard deviation (SD).

3. Results and discussion

The sample-level hierarchically gradient ultrafine-scale dislocation structure was introduced in face-centered cubic $Al_{0.1}CoCrFeNi$ HEA rods subjected to cyclic torsion (Figure 1). The representative microstructures of the three structural components in Figure 1(a) are shown in Figure 1(b–e) (at 0.6–1.2 mm depth), 1f–I (at 1.8–2.4 mm depth) and 1j–l (at sample core). After CT treatment, the polycrystalline grains are still homogeneously distributed

in these three structural components, where the polycrystalline grains are still tens of micron-scale in size ($\sim$46 μm), with unchanged morphologies and random orientation (Figure 1(b,f), analogous to that in the core or initial grain feature before cyclic torsion treatment (Figure 1(j)). Specifically, plenty of low-angle boundaries (LABs) are widely generated in grain interiors at the depth of 0.6–1.2 mm from top surface (Figure 1(c)). Further TEM observations reveal that numerous equiaxed dislocations cells and cell walls, with an average cell diameter of $\sim$0.29 μm are built in the surface grain interior (Figure 1(d–e)), corresponding to massive LABs.

With increasing depth to 1.8–2.4 mm depth from surface, equiaxed dislocation cells are rarely detected. Instead, undeveloped elongated dislocation cells, essentially composed of almost mutually intersected dislocation walls with a larger average spacing of $\sim$0.43 μm are universally detected, as shown in Figure 1(h,i). By contrast, few LABs with only several individual parallel dislocation traces along the 111 orientation exist in the grains of core component. Considering their almost homogeneous dislocation pattern distribution in dog-bone tensile specimens with average cell sizes of 0.29 and 0.43 μm, these two types of specimens are hereafter referred to as HDC-0.29 and HDC-0.43 components, respectively. The FG core containing few dislocations, with an average grain size of 46 μm, is also named as FG-46 specimen, for comparison.

Quasi-static uniaxial tensile tests of both free-standing HDCs show remarkably elevated mechanical properties. As shown in Figure 2(a), the measured yield strength evidently increases from $\sim$480 MPa for HDC-0.43 to $\sim$570 MPa for HDC-0.29 sample, 2–3 times as large as that of FG-46 counterpart, and even higher than that of bulk GDS sample ($\sim$540 MPa). Unexpected, good uniform elongation was identified in both HDC samples: $\sim$28.4% and $\sim$23.6% for HDC-0.43 and HDC-0.29 samples, respectively. However, the uniform plasticity maintained in both HDC units is still much lower than that ($\sim$43%) of gradient dislocation structure [19,20]. Such a strong-and-ductile tensile behavior of HDC foils is fundamentally distinct from the common mechanical performance trade-off trend in traditional UFG metals with almost the same characteristic size but massive high-angle GBs, i.e. strength gains at the cost of ductility loss [6–8]. The detailed tensile properties are summarized in Table 1.

Figure 2(b) presents the variation in the work-hardening rates ($\Theta = d\sigma/d\epsilon$) of both HDC specimens as a function of true strain. Notably, HDC-0.29 exhibits a smaller Θ than that of HDC-0.43 at the same strain, both of which are lower than that of GDS and FG-46

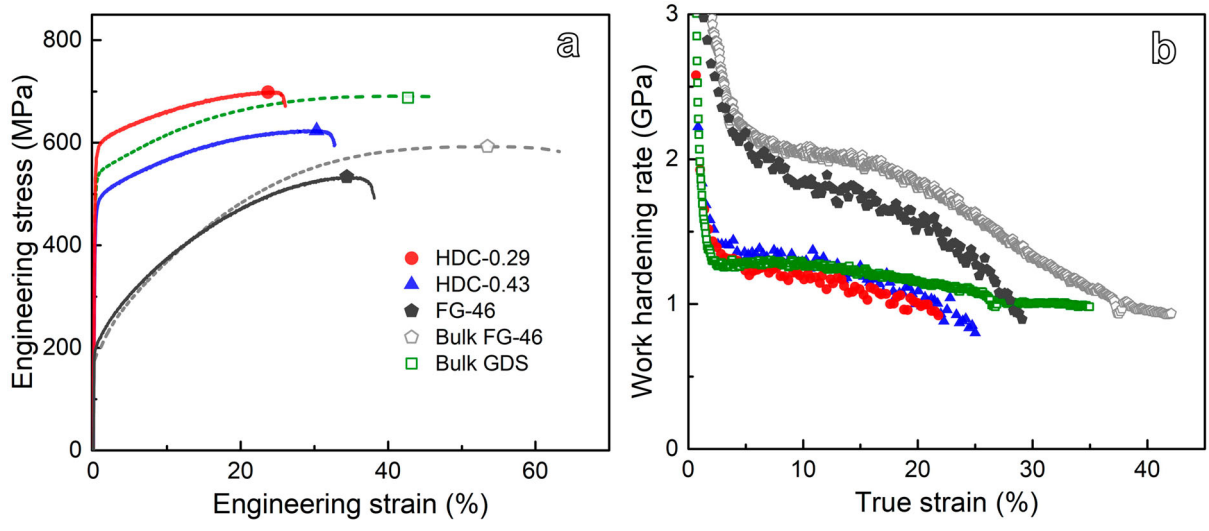

Figure 2. Mechanical properties of HDC structures. Tensile engineering stress-strain relations (a) and work-hardening rate versus true strain (b) of HDC and FG-46 foil samples compared with bulk GDS and FG samples.

Table 1. Tensile properties of HDC, FG-46 and GDS samples. σ_y, yield stress; σ_{UTS}, ultimate tensile strength; δ_u, uniform elongation; Hv, microhardness.

Sample	Structural size (μm)	σ_y (MPa)	σ_{UTS} (MPa)	δ_u (%)	*Hv* (GPa)
HDC-0.29	0.29 ± 0.09	567 ± 22	676 ± 29	23.6 ± 7.7	2.96 ~ 3.03
HDC-0.43	0.43 ± 0.15	479 ± 7	629 ± 7	28.4 ± 2.8	2.55 ~ 2.59
FG-46	46 ± 16	201 ± 5	529 ± 11	36.1 ± 1.6	2.17 ± 0.06
Bulk FG-46	46 ± 16	185 ± 5	599 ± 9	55.4 ± 3.4	1.82 ± 0.06
Bulk GDS	0.20 ~ 0.45	539 ± 26	689 ± 2	42.6 ± 0.2	3.76 ~ 2.31

in the entire strain stage. Nevertheless, both HDC components show a slightly, monotonically reduced Θ trend after the initial elastic-plastic transition strain (less than 1%), throughout the entire straining stage, which is distinct from the notably reduced work hardening in FG-46 and relatively steady work hardening trend in the GDS [19].

Microhardness (*H*v) measurements show that the presence of massive dislocation cell structure substantially improves the *H*v of HDC samples (Figure 3). For instance, a *H*v range from 2.59 GPa to 2.55GPa is identified in HDC-0.43 and a larger *H*v value from 3.03 GPa to 2.96 GPa for HDC-0.29, both of which are much higher than that (2.2 GPa) of FG-46 substrate. Such an almost homogeneous *H*v distribution in both HDC-0.29 and HDC-0.43 components further demonstrates a negligible through-thickness structural gradient exists in the prepared dog-bone tensile specimens. The *Hv* values in HDCs are approximately comparable to that in GDS sample with a diameter of 4.5 mm, essentially because the imposed torsion plastic strain accumulation on the bar sample tends to be the same for any position at the proportional depth (which scales to the gauge length) to the core under the same CT parameters [19].

As explicitly shown in Figure 3, the continuous hardening occurs in both HDC samples after tensile failure, consistent with tensile results (Figure 2). The microhardness of post-fracture HDC-0.29 sample increases from 2.99 GPa before tension to 3.62 GPa, which is slightly larger than that in HDC-0.43 sample (from 2.57 GPa to 3.35 GPa). Evidently, *Hv*s in tensiled HDC samples are still much lower than that of GDS counterpart (∼4.03–4.11 GPa) at a true strain of 34% at the same depth layer, indicative of the occurrence of extra hardening in these components when gradiently patterning in GDS. The continuous hardening feature, together with slightly reduced work hardening rate and good ductility, indicating an unusual deformation mechanism in homogeneous dislocation structure upon straining.

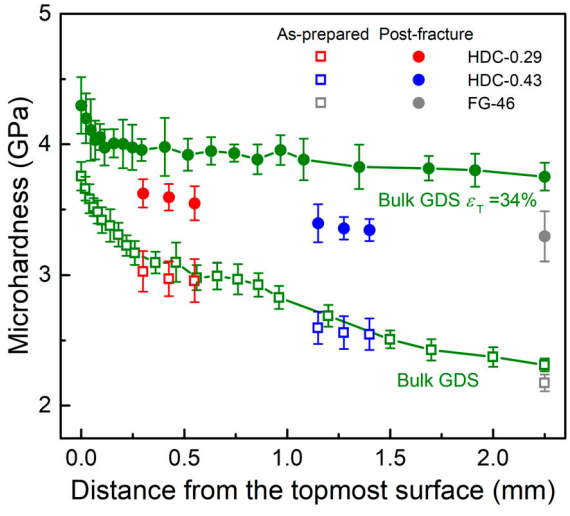

Figure 3. Microhardness tests in HDC, FG-46 and their post-fracture samples. Microhardness values of GDS and those after a 34% tensile true strain (ϵ_T) are also included for comparison.

To unravel the intrinsic deformation mechanism, the microstructural changes of the post-fracture HDC samples were systematically investigated by SEM and TEM. As shown in Figure 4(a–b) for tensiled HDC-0.29 samples, the initial regular dislocation cells (Figure 1(d)) before tension disappeared. Instead, denser irregular dislocation walls and loose tangles are prevalently observed in most grains. Furthermore, micro-scale elongated, parallel lamellar bundles with an average spacing of ∼4.3 μm have been sporadically detected within numerous grain interiors. Those lamellar bundles account for around 25% of the total grain count. Primarily stacking faults (SFs), with a few twin boundaries (TBs) in bundles are confirmed through selected-area electron diffraction (SAED) in Figure 4(c). High-magnification TEM image (Figure 4(d)) further reveals that each individual long lamellar bundle contains numerous tiny SFs and TBs, ranging from several to tens of nanometers in both length and spacing. The average thickness between adjacent SFs or TBs in the SF bundles is determined to be 7.9 nm, which remains smaller than that observed in GDS after tensile deformation.

By contrast, dense planar slip dislocation bands, without any detectable stacking faults and twins bundles, were detected in HDC-0.43 after tensile failure (Figure 4(e–f)). These foregoing results indicate that the configuration modification of dislocation patterns associated with the dominance of full dislocations and SF activities dominate the plastic deformation and contribute to the elevated strength and ductility combination in HDC HEA samples.

The high strength of HDC structures is essentially attributed to the ultrafine-scale dislocation cell structure with LABs. As the elementary linear defect with local varied strain/stress field, mutual dislocation interactions are known to induce the enhanced friction resistance to motion or accumulation of surrounding dislocations; dislocation strengthening is believed to approximately scale to the pre-existing dislocation density, according to the Taylor law [1,13]. As for both HDC samples, the presence of high density of dislocations themselves tends to induce remarkable strengthening. In addition, previous experiments and simulations have demonstrated that LABs themselves can also strengthen metals as effectively as conventional high-angle GBs [13,28]. Consequently, by decreasing the cell size into ultrafine scale, both unique structural features of HDC component, including a finer

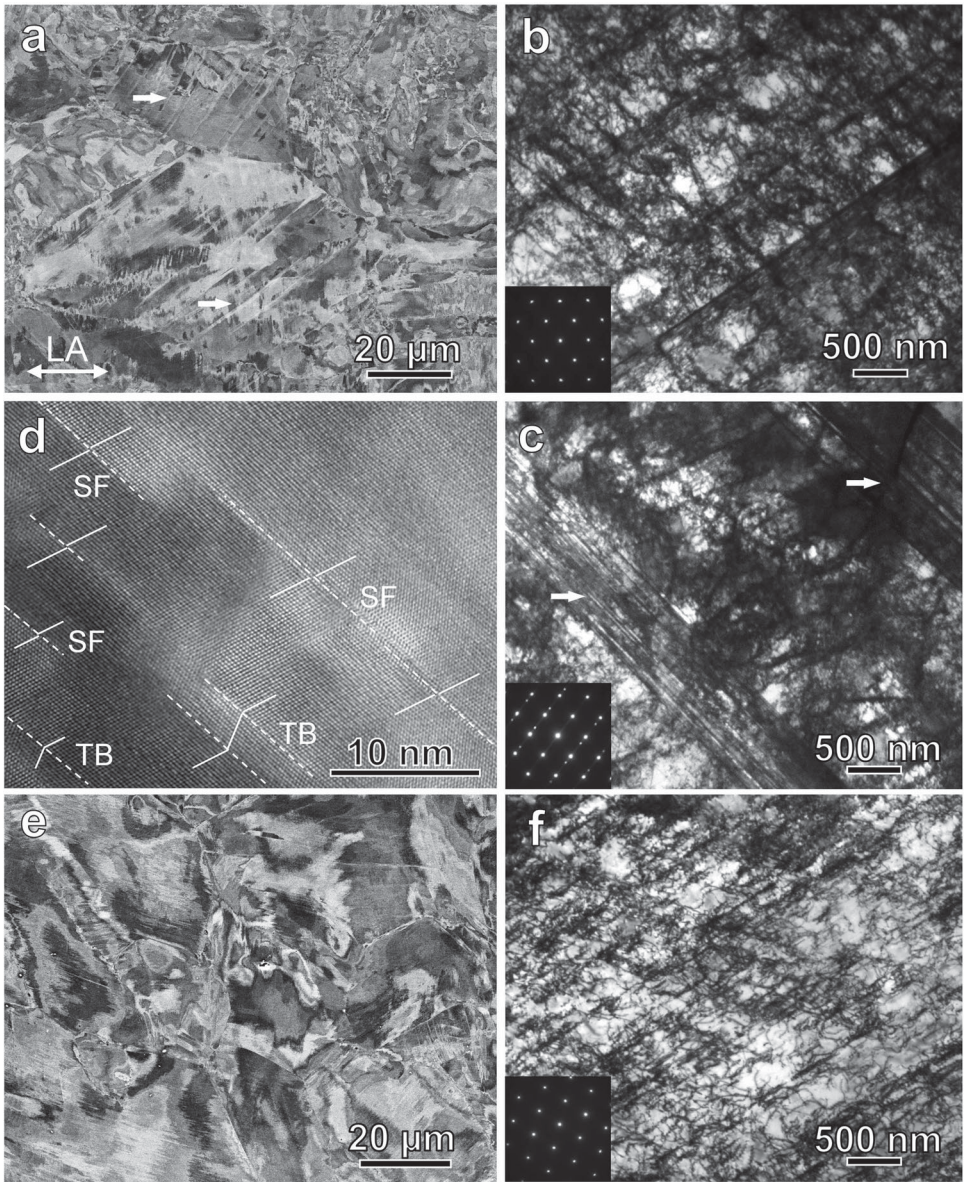

Figure 4. Deformed microstructure of HDC structures. SEM image (a), TEM images (b, c) and High resolution TEM image (d) in HDC-0.29 sample at a true strain of 24%, showing the evolved dislocation patterns, coupled with numerous SFs and twins (indicated by the white arrows). (e) and (f) exhibiting the dominance of planar slip structure of full dislocations in HDC-0.43 sample at a true strain of 27%.

structural size with LABs and a higher density of dislocations, can strongly block the inter-cell dislocation motion upon tensile straining, thereby leading to the elevated hardness and yield strength (Figures 2 and 3). That explains why a larger strength is achieved in HDC-0.29, compared to HDC-0.43 and FG-46.

The considerable ductility and work hardening also arise from beneficial contribution of the ultrafine-scaled dislocation patterns built in HEA. For traditional ultrafine grains under deformation, dislocations generate quickly from one GB, yet annihilate into other GBs, with little chance to be retained inside [7,8,13]. By contrast, one salient feature of HDC samples in this study is the presence of a high density of dislocations at walls, reasonably providing sustainable source for intra-grain dislocation nucleation. Under such circumstances, massive mutual interaction among full and partial dislocations and accumulation takes place to mediate the plastic strain in HDC units.

In addition, the motion of dislocation in HEA samples with inherent compositional heterogeneity has been demonstrated to be sluggish, more potentially promoting dislocation interaction, interlocking and accumulation, compared to conventional metals [15,29,30]. Distinct from the grain boundary migration associated with grain growth and resultant softening for nanograined

metals under plastic deformation, the ultrafine-sized dislocation cells built-in the coarse grains of HDC samples after CT treatment tend to be stable in a low energy state, owing to their feature of low-angle misorientations [1]. Consequently, the initial stable dislocation cells potentially undergo gradual configuration changes into dense intersected dislocation walls, rather than obvious structural coarsening, as shown in Figure 4(b,f). With further straining, the resultant progressive structural refinement associated with more intensive dislocation interactions and additional SF/twins act as more effective barriers to block dislocation motion, thus inducing considerable strengthening and strain hardening. This process can greatly counteract the rapidly decreased Θ of HDC structure that was inherently induced by the rapid recovery of pre-existing dislocations. That explains why a lower Θ at early strain is identified in HDC-0.29, compared to HDC-0.43 at the low strain.

Several SFs and twin bundles were solely detected in HDC-0.29 (Figure 4(c,d)), rather than in HDC-0.43 (Figure 4(f)), possibly owing to the strong size dependence of dislocation activities [2,31,32]. The activation of partial dislocations associated with SFs tends to become more favorable in HEAs containing a smaller-sized cell patterns [19,31]. Nevertheless, the SFs induced plasticity mechanism reported in GDS under tension is not the dominant strain carrier in free-standing HDC units.

The different deformation mechanisms in HDC and GDS samples most possibly arise from the contribution of the dislocation cell gradient. The considerably large structural gradient inherent in gradient DC samples plays a vital role in endowing progressive plastic deformation and effectively suppressing the overall strain localization [11,14,33]. Consequently, this process tends to result in plastic strain gradient and multiple-axial stress state for activating SFs mechanism in GDS samples. In addition, the above results further demonstrate that gradient manipulation of homogeneous dislocation patterns with different size scales can result in new SFs deformation mechanism and extra high hardening, thereby contributing to the higher uniform elongation and better strength and ductility combination in GDS samples. It has to be emphasized here that the measured uniform elongation of FG foil with the same geometry size as HDC samples (36%) is much lower than that (55%) of bulk FG counterpart [19] (Table 1), indicating that the sample geometry/size effect may underestimate the intrinsic ductility of HDC, worth of in-depth study in the future.

4. Conclusion

In summary, our study reveals that high yield strength and considerable uniform elongation larger than 24% are simultaneously achieved in homogeneous ultrafine-sized dislocation cell components with low-angle boundaries, in distinct contrast to the common strong-yet-less ductile ultrafine-grained structures with high angle grain boundaries. Such an unexpected mechanical property essentially stems from the progressive configuration evolution from the initial stable dislocation cells to dense dislocation walls associated with the motion and accumulation of massive dislocations. These findings deepen our understanding of mechanical behavior of low-angle-structured dislocation cell structure and provide a new promising pathway of developing high-performance metallic materials, by spatially tailoring nanosized dislocation patterns.

Disclosure statement

No potential conflict of interest was reported by the author(s).

Funding

Q. Pan and L. Lu acknowledge the financial support by the National Science Foundation of China [NSFC, Grant Numbers. 51931010, 92163202, 52122104 and 52071321], the Key Research Program of Frontier Science and International partnership program [GJHZ2029], IMR Innovation Fund [2022-ZD02] and Youth Innovation Promotion Association, Chinese Academy of Sciences [2019196].

References

[1] Meyers MA, Chawla KK. Mechanical behavior of materials. 2nd ed. Cambridge: Cambridge University Press; 2009.
[2] Hirth JP, Lothe J. Theory of dislocations. 2nd ed. New York: Wiley; 1982.
[3] Lu L, Chen X, Huang X, et al. Revealing the maximum strength in nanotwinned copper. Science. 2009;323:607–610. doi:10.1126/science.1167641
[4] Lu K, Lu L, Suresh S. Strengthening materials by engineering coherent internal boundaries at the nanoscale. Science. 2009;324:349–352. doi:10.1126/science.1159610
[5] Gleiter H. Nanocrystalline materials. Prog Mater Sci. 1989;33:223–315. doi:10.1016/0079-6425(89)90001-7
[6] Koch CC, Morris DG, Lu K, et al. Ductility of nanostructured materials. MRS Bull. 1999;24:54–58. doi:10.1557/S0883769400051551
[7] Kumar KS, Van Swygenhoven H, Suresh S. Mechanical behavior of nanocrystalline metals and alloys11The golden jubilee issue—selected topics in materials science and engineering: past, present and future, edited by S. Suresh. Acta Mater. 2003;51:5743–5774. doi:10.1016/j.actamat.2003.08.032
[8] Meyers MA, Mishra A, Benson DJ. Mechanical properties of nanocrystalline materials. Prog Mater Sci. 2006;51:427–556. doi:10.1016/j.pmatsci.2005.08.003
[9] Fang TH, Li WL, Tao NR, et al. Revealing extraordinary intrinsic tensile plasticity in gradient nano-grained copper. Science. 2011;331:1587–1590. doi:10.1126/science.1200177

[10] Wei YJ, Li Y, Zhu L, et al. Evading the strength-ductility trade-off dilemma in steel through gradient hierarchical nanotwins. Nat Commun. 2014;5:3580, doi:10.1038/ncomms4580
[11] Wu XL, Jiang P, Chen L, et al. Extraordinary strain hardening by gradient structure. Proc Natl Acad Sci U S A. 2014;111:7197–7201. doi:10.1073/pnas.1324069111
[12] Wu XL, Yang MX, Yuan FP, et al. Heterogeneous lamella structure unites ultrafine-grain strength with coarse-grain ductility. Proc Natl Acad Sci U S A. 2015;112:14501–14505. doi:10.1073/pnas.1517193112
[13] Lu K. Stabilizing nanostructures in metals using grain and twin boundary architectures. Nat Rev Mater. 2016;1:16019, doi:10.1038/natrevmats.2016.19
[14] Li XY, Lu L, Li JG, et al. Mechanical properties and deformation mechanisms of gradient nanostructured metals and alloys. Nat Rev Mater. 2020;5:706–723. doi:10.1038/s41578-020-0212-2
[15] Sathiyamoorthi P, Kim HS. High-entropy alloys with heterogeneous microstructure: processing and mechanical properties. Prog Mater Sci. 2022;123:100709, doi:10.1016/j.pmatsci.2020.100709
[16] Wang F, Li Y, Chen X, et al. Superior strength-ductility combination in Al alloys via dislocation gradient structure. Mater Res Lett. 2023;11:347–353. doi:10.1080/21663831.2022.2151851
[17] Zhu YT, Ameyama K, Anderson PM, et al. Heterostructured materials: superior properties from hetero-zone interaction. Mater Res Lett. 2021;9:1–31. doi:10.1080/21663831.2020.1796836
[18] Pan QS, Guo S, Cui F, et al. Superior strength and ductility of 304 austenitic stainless steel with gradient dislocations. Nanomaterials. 2021;11:2611–2619. doi:10.3390/nano11102613
[19] Pan QS, Zhang LX, Feng R, et al. Gradient cell–structured high-entropy alloy with exceptional strength and ductility. Science. 2021;374:984–989. doi:10.1126/science.abj8114
[20] Pan QS, Lu L. Synthesis and deformation mechanics of gradient nanostructured materials. Nation Sci Open. 2022;1(1):20220010. doi.org/10.1360/nso/20220010.
[21] Lin Y, Pan J, Zhou HF, et al. Mechanical properties and optimal grain size distribution profile of gradient grained nickel. Acta Mater. 2018;153:279–289. doi:10.1016/j.actamat.2018.04.065
[22] Long JZ, Pan QS, Tao NR, et al. Improved fatigue resistance of gradient nanograined Cu. Acta Mater. 2019;166:56–66. doi:10.1016/j.actamat.2018.12.018
[23] Wang JJ, Tao NR, Lu K. Revealing the deformation mechanisms of nanograins in gradient nanostructured Cu and CuAl alloys under tension. Acta Mater. 2019;180:231–242. doi:10.1016/j.actamat.2019.09.021
[24] Li W, Xie D, Li D, et al. Mechanical behavior of high-entropy alloys. Prog Mater Sci. 2021;118:100777, doi:10.1016/j.pmatsci.2021.100777
[25] Herzog D, Seyda V, Wycisk E, et al. Additive manufacturing of metals. Acta Mater. 2016;117:371–392. doi:10.1016/j.actamat.2016.07.019
[26] Wang YM, Voisin T, McKeown JT, et al. Additively manufactured hierarchical stainless steels with high strength and ductility. Nat Mater. 2018;17:63–71. doi:10.1038/nmat5021
[27] Li J, Yi M, Wu H, et al. Fine-grain-embedded dislocation-cell structures for high strength and ductility in additively manufactured steels. Mater Sci Eng, A. 2020;790:139736, doi:10.1016/j.msea.2020.139736
[28] Liu XC, Zhang HW, Lu K. Strain-induced ultrahard and ultrastable nanolaminated structure in nickel. Science. 2013;342:337–340. doi:10.1126/science.1242578
[29] Ma E. Unusual dislocation behavior in high-entropy alloys. Scr Mater. 2020;181:127–133. doi:10.1016/j.scriptamat.2020.02.021
[30] Yeh JW. Chapter 3. Physical metallurgy. In: Gao MC, Yeh JW, Liaw PK, Zhang Y, editor. High-Entropy alloys fundamentals and applications. Switzerland: Springer International; 2016. p. 51–113.
[31] Orowan E. The symposium on internal stresses in metals and alloys. London: Institute of Metals; 1948. p. 451.
[32] Asaro RJ, Krysl P, Kad B. Deformation mechanism transitions in nanoscale fcc metals. Philos Mag Lett. 2003;83:733–743. doi:10.1080/09500830310001614540
[33] Ashby MF. The deformation of plastically non -homogeneous materials. Philos Mag. 1970;21:399–424. doi:10.1080/14786437008238426